



Missouri University of Science and Technology
Scholars' Mine

Electrical and Computer Engineering Faculty
Research & Creative Works

Electrical and Computer Engineering

01 Mar 2006

Direct Torque Control of Five-Phase Induction Motor Using Space Vector Modulation with Harmonics Elimination and Optimal Switching Sequence

Shuai Lu

Keith Corzine

Missouri University of Science and Technology

Follow this and additional works at: https://scholarsmine.mst.edu/ele_comeng_facwork

 Part of the [Electrical and Computer Engineering Commons](#)

Recommended Citation

S. Lu and K. Corzine, "Direct Torque Control of Five-Phase Induction Motor Using Space Vector Modulation with Harmonics Elimination and Optimal Switching Sequence," *Proceedings of the Twenty-First Annual IEEE Applied Power Electronics Conference and Exposition, 2006. APEC '06*, Institute of Electrical and Electronics Engineers (IEEE), Mar 2006.

The definitive version is available at <https://doi.org/10.1109/APEC.2006.1620539>

This Article - Conference proceedings is brought to you for free and open access by Scholars' Mine. It has been accepted for inclusion in Electrical and Computer Engineering Faculty Research & Creative Works by an authorized administrator of Scholars' Mine. This work is protected by U. S. Copyright Law. Unauthorized use including reproduction for redistribution requires the permission of the copyright holder. For more information, please contact scholarsmine@mst.edu.

Direct Torque Control of Five-Phase Induction Motor Using Space Vector Modulation with Harmonics Elimination and Optimal Switching Sequence

Shuai Lu, *Student Member, IEEE*, and Keith Corzine, *Member, IEEE*

Department of Electrical Engineering, University of Missouri - Rolla
1870 Miner Circle, Rolla, MO 65401-0040

Abstract - In this paper an effective direct torque control (DTC) for a 5-phase induction motor with sinusoidally distributed windings is developed. First by coordinate transformation, the converter/motor models are represented by two independent equivalent d - q circuit models; and the 5-phase VSI input are decoupled into the torque producing and non-torque producing harmonics sets. Then with the torque production component of the induction motor model, the space vector modulation (SVM) can be applied to the five-phase induction motor DTC control, resulting in considerable torque ripple reduction over the lookup table method. Based on the decoupled system model, the current distortion issue due to lack of back EMF for certain harmonics is analyzed. Two equally effective SVM schemes with the harmonic cancellation effect are introduced to solve this problem. To analyze the DTC control torque ripple, an insightful perspective (also applicable to 3-phase analysis) is introduced to predict the torque ripple pattern evolution with changing motor speed and stator flux angular position. Therefore the switching sequence for lowest torque ripple can be determined and re-arranged online. Finally, with the overall optimal switching scheme adopted, detailed simulations verify the effectiveness of the new control.

I. INTRODUCTION

Direct torque control (DTC) [1-5] has been gaining more popularity since its introduction due to its exceptional dynamic response and less dependence on machine parameters. It has been applied to the multi-phase motor (with high reliability and power density) [6, 7], in which DTC with a lookup table is used to control 5-phase induction motor [6] and a PMSM [7] with concentrated stator windings. Due to the abundance of voltage vectors in the 5-phase drive system, steady-state torque ripple performance showed considerable improvement over comparable 3-phase drives.

The first contribution of this paper is to replace the lookup table DTC with the DTC space vector modulation (DTC-SVM) in the 5-phase IM drive. This type of control further reduces the torque ripple because it can produce the voltage reference which accurately compensates the differences between the commanded torque/flux values and their actual values from measurement and estimation. The look up table DTC, uses alternatively "forward" and "backward" active vectors to bring the flux and torque within the hysteresis band. For the lookup table DTC, the analog hysteresis control has the issue of varying switching frequency but its torque ripple can be controlled by setting the hysteresis band; the digital hysteresis implementation has a fixed switching frequency, but the larger torque ripple become an issue.

Moreover, it is shown in the paper that in 5-phase motors with sinusoidally distributed stator windings, the absence of back EMF for non-torque-producing harmonics (mostly the 3rd harmonic) will result in considerable harmonic current, if the modulation scheme can't completely cancel out such voltage harmonics using the VSI inverter. This causes deformation of the phase current and extra copper losses (while not causing torque pulsation). For sinusoidal results, the lookup table DTC and even the DTC using SVM (with one pair of closest vectors plus the zero-vector) can't be used in a sinusoidally wound 5-phase motor. At least two pairs of voltage vectors with the zero-vector are required for the harmonic free operation. Two such SVM schemes are introduced in this paper.

The last part of this paper systematically addresses several concepts such as how to evaluate if certain switching sequence (vector sequence) will achieve minimal torque ripple, analytically predicting the torque ripple pattern without simulation, and the torque ripple shape as motor speed changes.

II. FIVE-PHASE MOTOR/CONVERTER MODELING IN $dq1$ AND $dq2$ PLANES

For the 5-phase inverter/motor system (shown in Figure 1), 5-dimensional machine variables can be transformed into $d1$ - $q1$ and $d2$ - $q2$ reference frames and a zero sequence variable [8]. The resulting two-dimensional $d1$ - $q1$ plane is aligned with the physical rotating flux plane and its equivalent circuit appears the same as the d - q model of 3-phase motor (shown in Figure 2). The fundamental component and the harmonics of order $10n \pm 1$ ($n=1, 2, 3, \dots$) are applied on the $d1$ - $q1$ plane circuit to produce a rotating MMF and torque (harmonics produce torque pulsation). The harmonics of order $5n \pm 2$ ($n=1, 3, 5, \dots$) (non-torque producing) are applied onto the remaining $d2$ - $q2$ plane and its equivalent circuits after transformation have only winding resistance and leakage inductance (Figure 2) so that the $d2$ - $q2$ plane harmonic current could be large even with small voltage input. The harmonic currents in $d2$ - $q2$ plane, if exist, are then superimposed onto the phase current by inverse transformation and lead to current deformation and extra copper loss in the motor. However, the highly distorted phase current by the $d2$ - $q2$ plane harmonics will not deform the MMF and resulting torque output, as long as the VSI inverter produces no low-order harmonics in the $d1$ - $q1$ plane.

For a 5-phase induction motor fed by two-level VSI converters, the line-to-ground voltage can be calculated using

$v_{kg} = s_k v_{dc}$ where $k = a, b, c, d, e$ and s_k is the per-phase switching state having a range of $s_k = 0, 1$. The line-to-neutral voltage can be expressed by:

$$\begin{bmatrix} v_{as} \\ v_{bs} \\ v_{cs} \\ v_{ds} \\ v_{es} \end{bmatrix} = \frac{1}{5} \begin{bmatrix} 4 & -1 & -1 & -1 & -1 \\ -1 & 4 & -1 & -1 & -1 \\ -1 & -1 & 4 & -1 & -1 \\ -1 & -1 & -1 & 4 & -1 \\ -1 & -1 & -1 & -1 & 4 \end{bmatrix} \begin{bmatrix} v_{ag} \\ v_{bg} \\ v_{cg} \\ v_{dg} \\ v_{eg} \end{bmatrix} \quad (1)$$

The line-to-neutral voltages can be transformed to the d - q planes using the following transformation matrix [8]:

$$K = \frac{2}{5} \begin{bmatrix} \cos \theta & \cos(\theta - \frac{2}{5}\pi) & \cos(\theta - \frac{4}{5}\pi) & \cos(\theta + \frac{4}{5}\pi) & \cos(\theta + \frac{2}{5}\pi) \\ \sin \theta & \sin(\theta - \frac{2}{5}\pi) & \sin(\theta - \frac{4}{5}\pi) & \sin(\theta + \frac{4}{5}\pi) & \sin(\theta + \frac{2}{5}\pi) \\ \cos \theta & \cos(\theta + \frac{4}{5}\pi) & \cos(\theta - \frac{2}{5}\pi) & \cos(\theta + \frac{2}{5}\pi) & \cos(\theta - \frac{4}{5}\pi) \\ \sin \theta & \sin(\theta + \frac{4}{5}\pi) & \sin(\theta - \frac{2}{5}\pi) & \sin(\theta + \frac{2}{5}\pi) & \sin(\theta - \frac{4}{5}\pi) \\ \frac{1}{2} & \frac{1}{2} & \frac{1}{2} & \frac{1}{2} & \frac{1}{2} \end{bmatrix} \quad (2)$$

Note that (2) is also used to transform the motor model into the $d1$ - $q1$ and $d2$ - $q2$ plane equivalent circuits as in Figure 2. Thirty two voltage vectors (switching states) of the 5-phase VSI inverter are transformed into the two planes as shown in Figure 3 as dual decagon patterns. Note that all the voltage vectors along the outer-ring in $d1$ - $q1$ plane are located in the inner rings of the $d2$ - $q2$ and vice versa. Then the same set of voltage vectors are in the mid-ring of both decagons. While any type of PWM frequency modulation in the $d1$ - $q1$ plane produce no low frequency harmonics (causing low frequency torque pulsation); to keep the average voltage (harmonics voltages) in $d2$ - $q2$ plane to be zero, proper vector selection and timing ratio should be used [9] [11].

Consider what happens if a single pair of vectors plus a zero-vector are used to produce the reference with a circular locus in the $d1$ - $q1$ plane. In Figure 4(a), the corresponding space vector locus (fast average value) is plotted in the $d2$ - $q2$ plane. The locus shape indicates the combination of 3rd and 7th harmonics. In the time domain, the 3rd and 7th voltage harmonics, as in Figure 4(b), will superpose onto the fundamental component in $d1$ - $q1$ plane and the phase voltage/current (v_{as} and i_{as}) will thus be deformed. Since the fundamental voltage and 3rd and 7th harmonic voltages apply to different equivalent circuits, the harmonic current will have a different phase shift. The rated load fundamental current will lag the voltage by $\cos^{-1}(0.8)$ (assuming a power factor of 0.8) and 3rd and 7th harmonics current will lag by almost 90° (assuming stator resistance is negligible). Also the small impedance without back EMF terms in $d2$ - $q2$ plane circuit induces large magnitude harmonic current which is almost comparable to that of the fundamental. The simulation results shown in Figure 4(c) demonstrate the highly deformed phase current induced by small voltage harmonics from the $d2$ - $q2$

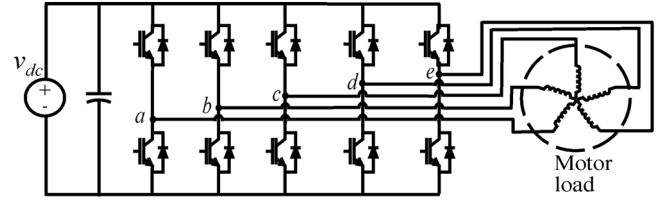


Figure 1. Five-phase motor drive.

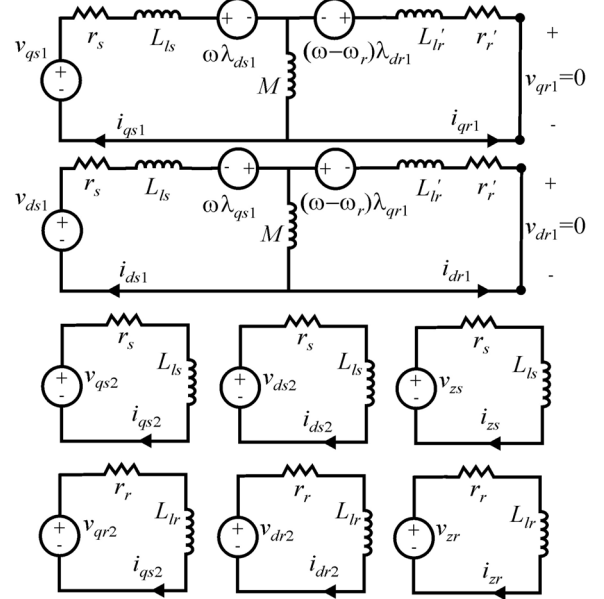


Figure 2. Five-phase induction motor equivalent circuits in $d1$ - $q1$, $d2$ - $q2$ planes and zero sequence variables.

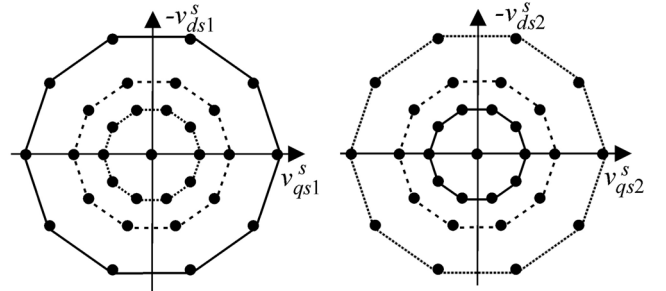


Figure 3. Voltage vectors in the $d1$ - $q1$ and $d2$ - $q2$ plane.

plane. The results match the above theoretical predictions well. Therefore the presence of the non-zero fast average voltage locus in the $d2$ - $q2$ plane should be somehow eliminated, which is equivalent to having zero vector sums in $d2$ - $q2$ plane within one PWM cycle. This constraint can be expressed as

$$\sum_{x=1}^n v_{x-d2-q2} \cdot D_x \cdot T_{DSP} = 0 \quad (3)$$

where n is the total number of active $d2$ - $q2$ plane vectors traversed per PWM cycle and $v_{x-d2-q2}$ represents each such voltage vector. The variable D_x is the vector duty ratio.

The DTC with lookup table implementation will not satisfy (3) since its vector selection is solely based on the hysteresis

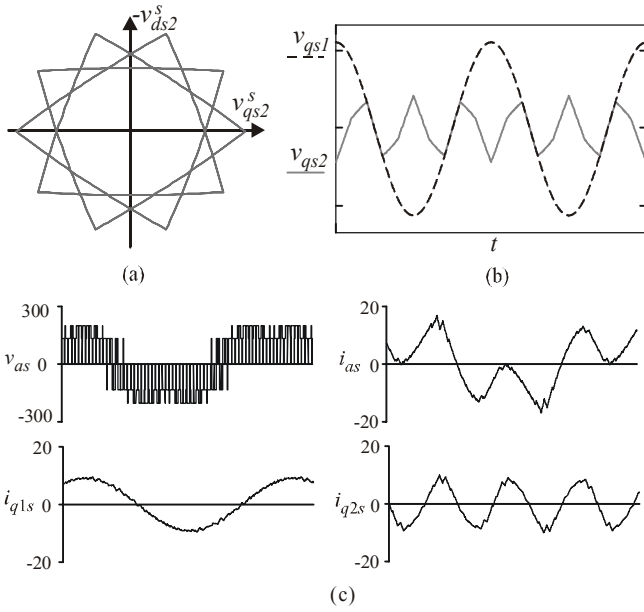


Figure 4 . Five-phase SVM with a single pair of vectors and its $d2-q2$ plane and corresponding voltage and current harmonics.

torque/flux comparison and then each vector is applied in one full DSP cycle. As discussed below, two pairs of active vectors are the minimal requirement to satisfy (3).

III. PROPOSED DTC-SVM IN THE 5-PHASE INDUCTION MOTOR DRIVE

Compared with the steady-state performance of lookup table DTC, DTC-SVM results in much lower torque ripple. This is because, it uses the zero-vector instead of backward active vectors to reduce torque. Also, it achieves exact balance of the torque increase/decrease within one DSP cycle, which is not guaranteed by lookup table DTC. Figuratively speaking, the lookup table DTC implicitly synthesizes a virtual voltage reference with a fast-average value fluctuating around the ideal value (assuming digital hysteresis implementation). This fluctuation induces extra torque ripple.

Figure 5 shows the block diagram of the proposed DTC-SVM in a 5-phase IM drive. In the torque producing $d1-q1$

plane, the torque and flux estimator equations are the same as the conventional 3-phase DTC drive, except for replacing 3/2 with 5/2 in torque equation. The specific flux and torque equations are:

$$\lambda_{qs} = \int_0^t (v_{qs} - i_{qs} \cdot r_s) \cdot dt \quad (4)$$

$$\lambda_{ds} = \int_0^t (v_{ds} - i_{ds} \cdot r_s) \cdot dt$$

$$T_e = \frac{5P}{2} (\lambda_{qs} i_{ds} - \lambda_{ds} i_{qs}) \quad (5)$$

To obtain the voltage reference for the SVM modulator, various methods exist [3-5]. Among them, dual PI-controllers adjusting the radial and tangential voltage vectors (relative to flux vector) is a straightforward option. Its resulting voltage reference vector is very accurate. As long as the reference is correct, the steady-state torque ripple performance is only dependent on the SVM vector selection and sequence, instead of the methods used to obtain the reference.

It can be noted that in Figure 5, only $d1-q1$ plane variables are used for DTC control reference voltage, the $d2-q2$ plane variables are commanded to be zero by SVM module to guarantee the vectors in $d2-q2$ plane cancel each other in one DSP cycle. This process is discussed in the following section.

IV. TWO SVM SCHEMES WITH HARMONIC FREE OPERATION

Two SVM schemes are introduced herein. Both are based on the principle to locate the nearest two pairs of voltage vectors in $d1-q1$ plane and find their proper duty ratios. As a result, the voltage reference in the $d1-q1$ plane is properly synthesized; while the same set of vectors satisfy (3) and completely cancel out each other in the $d2-q2$ plane. Therefore, no low-frequency harmonics exist in phase-to-neutral variables. As stated previously, at least two pairs of vectors are needed besides the zero-vector.

The first SVM scheme can be easily implemented as the natural sampling process with one sinusoidal PWM reference per phase leg. The vector set and their timing ratio selection are automatically done this way. As illustrated in Figure 6, when the reference is in sector 1 (0° , 36°), the four vectors

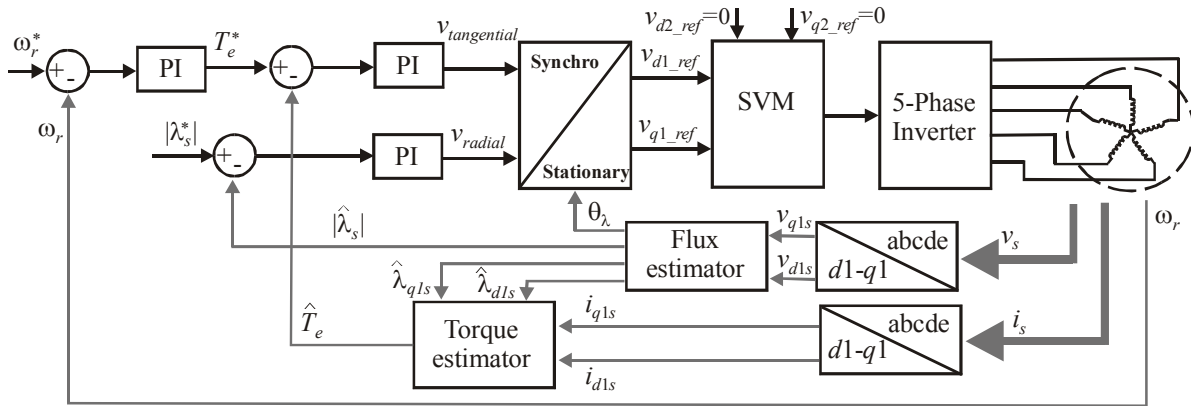


Figure 5. Proposed DTC-SVM control block diagram

(plus zero) in gray dots in $d1-q1$ plane synthesize the voltage reference, while canceling each other in $d2-q2$ plane. The time ratio between the outer ring vector and mid ring vector in $d1-q1$ (11000 vs. 11101 or 11001 vs. 10000) will always be 1.618:1. Since the amplitude ratio between the same pairs of vectors (in $d2-q2$ plane) is 1:1.618, the two pairs of vectors will satisfy (3) and have zero average voltage in the $d2-q2$ plane.

The second SVM scheme was applied to a 6-phase system in the literature [9] and can be adapted to a 5-phase system as shown in Figure 7. In the vector plot of $d1-q1$ plane, the four neighboring vectors spanning along the outer ring was selected. To guarantee zero average voltage in $d2-q2$ plane, the following set of four equations with four unknown time ratios needs to be solved:

$$\begin{bmatrix} d_1^1 & d_1^2 & d_1^3 & d_1^4 \\ q_1^1 & q_1^2 & q_1^3 & q_1^4 \\ d_2^1 & d_2^2 & d_2^3 & d_2^4 \\ q_2^1 & q_2^2 & q_2^3 & q_2^4 \end{bmatrix}^{-1} \begin{bmatrix} v_{d1_ref}/v_{dc} \\ v_{q1_ref}/v_{dc} \\ 0 \\ 0 \end{bmatrix} = \begin{bmatrix} t_1 \\ t_2 \\ t_3 \\ t_4 \end{bmatrix} \quad (6)$$

and $t_0 = 1 - (t_1 + t_2 + t_3 + t_4)$. In (6), t_x is the time ratio of vector v_x ; d_1^x , q_1^x and d_2^x , q_2^x are the projections of v_x onto the $d1-q1$ and $d2-q2$ axis. In a DSP implementation, the switching states and the inverse matrix of $d1-q1/d2-q2$ projections of these four vectors (v_1 to v_4) for sector 1 (0° to 36°) needs to be stored in memory. When the reference falls into other sectors, it can be normalized to sector 1 and the new set of four voltage vectors in a different sector (switching states) can be computed by straightforward cyclic rules.

V. OPTIMAL TORQUE RIPPLE AND SWITCHING SEQUENCE ANALYSIS

The DTC-SVM driven motor torque ripple patterns depend on many factors such as stator flux amplitude, reference voltage amplitude, motor synchronous speed, etc. Conventionally, the definite prediction of the ripple pattern can only be done by detailed simulation of the whole system. This section introduces an insightful method to approach the torque ripple from a space vector perspective. With the methodology introduced, the torque ripple patterns can be analytically predicted and it is then possible to find the optimal switching sequence to realize the lowest torque ripple. Note that the same methodology can also be applied to the 3-phase system SVM torque ripple analysis.

A. Stator Flux Rotation Speed and Amplitude Variation

In ideal steady-state operation, the stator flux λ_s and rotor flux λ_r vectors both rotate at the electric synchronous speed ω_s , with λ_s leading λ_r by the angle δ . The instantaneous torque is expressed as:

$$T_e = K \cdot |\lambda_r| \cdot |\lambda_s| \cdot \sin(\delta) \quad (7)$$

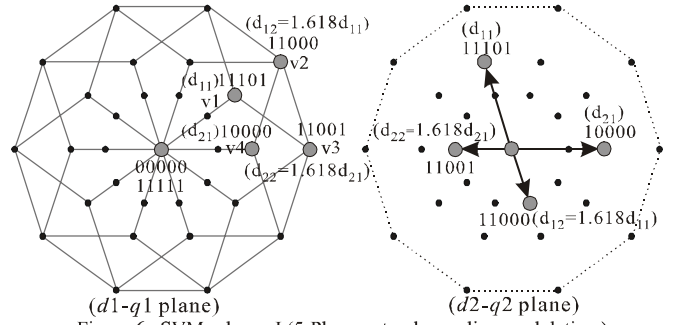


Figure 6. SVM scheme I (5-Phase natural sampling modulation).

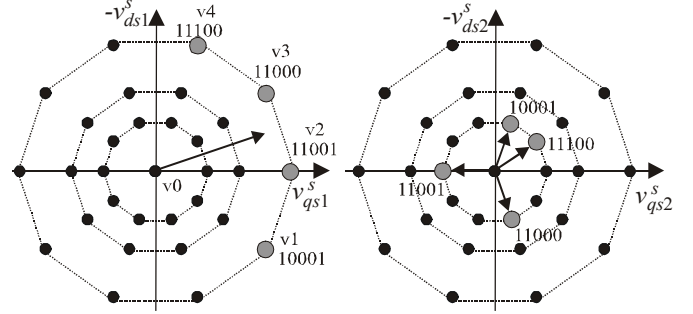


Figure 7. SVM scheme II (using two pairs of vectors along outer ring).

where K is a coefficient depending on the motor parameters. In an inverter-fed motor drive, the rotor flux rotation can still be regarded as constant speed due to its large time constant. However, the speed and the amplitude of the λ_s depend on currently applied voltage vector. The following equations calculate the λ_s instantaneous rotation speed and amplitude variation when a certain voltage vector is applied:

$$\omega_{\lambda_s} = \frac{v_{x,\tan-proj} \cdot D_x \cdot T_{DSP}}{D_x \cdot T_{DSP} \cdot |\lambda_s|} = \frac{v_{x,\tan-proj}}{|\lambda_s|} \quad (8)$$

$$\Delta |\lambda_s| = v_{x,\text{radial-proj}} \cdot D_x \cdot T_{DSP} \quad (9)$$

where $v_{x,\tan-proj}$ and $v_{x,\text{radial-proj}}$ are the voltage vector tangential and radial projections along the λ_s locus; D_x is the duty ratio of the voltage vector; $v_{x,\tan-proj} \cdot D_x \cdot T_{DSP}$ and $v_{x,\text{radial-proj}} \cdot D_x \cdot T_{DSP}$ are the tangential/radial displacement of the stator flux with the voltage vector, which is then divided by vector active time $D_x \cdot T_{DSP}$ and the stator flux magnitude $|\lambda_s|$ to get the instantaneous angular speed. The resulting ω_{λ_s} is either larger or smaller than ω_s (rotor flux speed). This changes the δ angle and the instantaneous torque fluctuates accordingly. Additionally, the $|\lambda_s|$ variation also affects the torque. As discussed next, the resulting torque ripple has different patterns depending on synchronous speed ω_s and the angular position of λ_s .

B. Torque Ripple Pattern Evolution and On-line Torque Slope Determination

As shown in Figures 8a1 and 8a2, the torque ripple is analyzed in the highlighted sector 1 for both SVM methods, and the results are applicable to all ten sectors. Assuming the resistive voltage drop in (4) is negligible, the flux λ_s and the VSI reference voltage vector v_s are 90° apart. The angle θ is the angle between the v_s and the lower boundary of the sector. As flux angular position, or θ , increases within the sector, the tangential projections of four active vectors used in each PWM cycle (in larger grey dots) will change, hence their instantaneous stator flux rotating speed ω_{λ_s} . In Figures 8b1 and 8b2, the ω_{λ_s} for four vectors are plotted along $0^\circ < \theta < 36^\circ$ for both SVM methods. The horizontal dotted line represents the rotor flux speed ω_s , which is adjusted by the DTC control. Depending on the ω_s and the stator flux angular position θ , the ω_{λ_s} of each voltage vector could be either higher or lower than ω_s . The torque angle variation $\Delta\delta$ is expressed as follows

$$\Delta\delta = (\omega_{\lambda_s} - \omega_s) \cdot D_x \cdot T_{DSP} \quad (10)$$

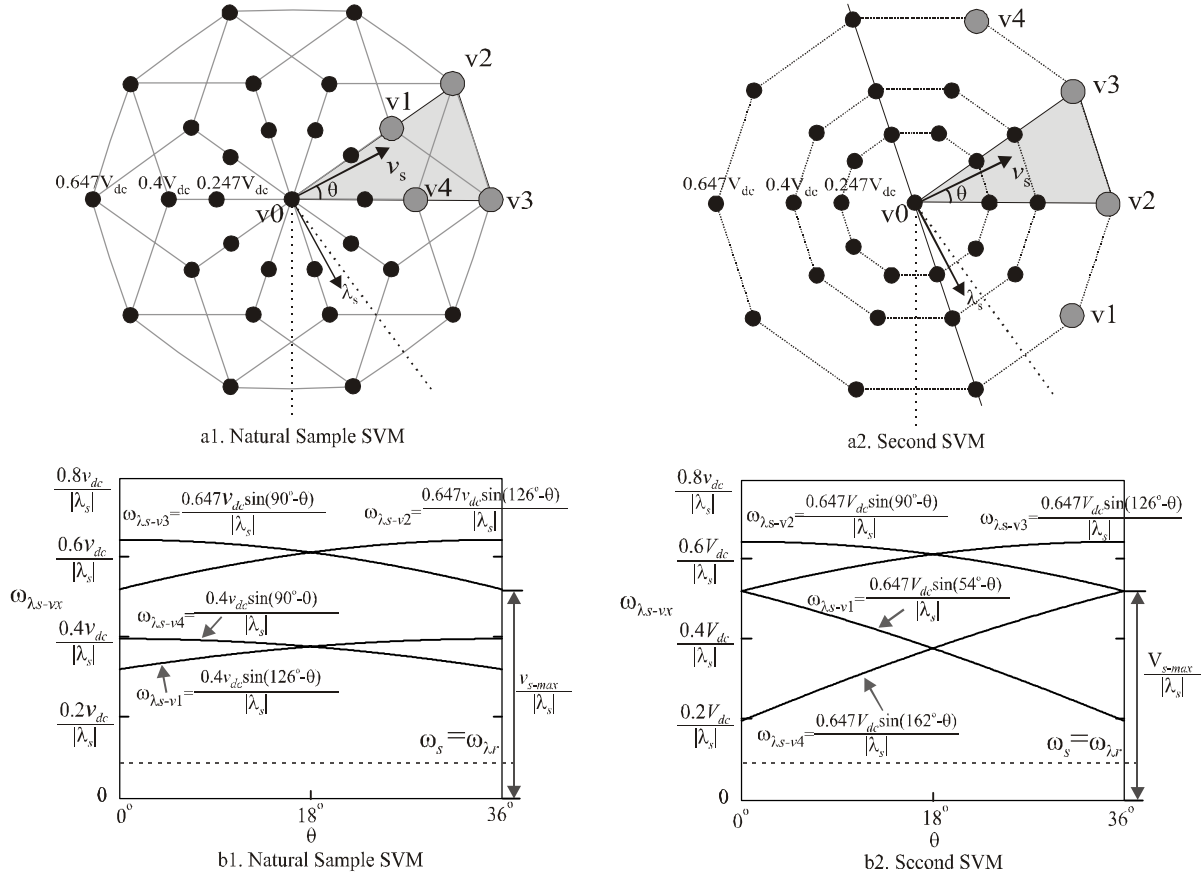


Figure 8. Torque ripple space vector analysis and its evolution over different speed and stator flux angular position.

To decide if the vector associated torque slope will be positive or negative, the $|\lambda_s|$ variation over the different angular position also needs to be considered. The set of curves similar to Figures 8b1 and 8b2 can also be plotted for $\Delta|\lambda_s|$ versus θ . Note that the absolute torque variation ΔT_e for each voltage vector is not the concern, only the torque slope direction matters for selecting a better vector sequence. Therefore, by comparing $(|\lambda_s| + \Delta|\lambda_s|) \cdot \sin(\delta + \Delta\delta)$ with $|\lambda_s| \cdot \sin(\delta)$, the torque slope direction can be determined dynamically in the DSP implementation.

C. Simplified Prediction of Torque Pattern Evolution

The above torque slope prediction method can be greatly simplified with following two facts. First, compared to torque angle variation, effects of the stator flux magnitude variation on the torque can be safely neglected; particularly at light load conditions (The proof of this fact is beyond the scope of the paper). So the torque slope direction for each vector can be directly found with Figures 8b1 and 8b2.

Secondly, for the total vectors cancellation in $d2-q2$ plane, the two pair of vectors has certain timing ratio between them. For example, in natural sample SVM, the timing ratio between v2 and v1 (or v3 and v4) is always 1.618:1. Therefore, the vector v2 and v3 has larger duty ratio than v1 and v4.

The normal motor speed range is designated in Figures 8b1

and 8b2. Obviously, for v_2 and v_3 , their $|\omega_{\lambda s} - \omega_s|$ value is much larger than that of the v_1 and v_4 . From (10), it is then concluded that the v_2 and v_3 will always create positive torque ramp and constitute the majority of torque increment in one PWM cycle. The torque decrement occurs when zero-vector is applied. The effects from v_1 and v_4 vectors can be ignored and regard as nearly “flat” torque ramps.

The Figure 9 shows the zoom-in view of the torque ripple simulation when the motor speed is low and high (at no-load). The vector v_1 and v_4 torque slope evolve from positive to negative as motor speed increases. But their effects can be obviously ignored as previously concluded.

D. Optimal Vector Sequence

The essence of the minimal torque ripple vector sequence is to reshuffle the order of the voltage vectors per DSP cycle to make the torque increase/decrease ramps sandwich each other. This way the maximum torque peak to peak value will only be equal to the largest torque variation with certain voltage vector, instead of the cascading of several ramps in the same direction. However, the minimal torque ripple sequence might not have minimal numbers of switching per PWM cycle.

For natural sampling SVM, the switching sequence is implicitly achieved by using the center-aligned triangular carrier. It has the lowest possible switching numbers (one per inverter state change). The vector sequence alternates between ($v_0(11111) - v_1 - v_3 - v_2 - v_4 - v_0(00000)$) and ($v_0(00000) - v_4 - v_2 - v_3 - v_1 - v_0(11111)$) as labeled in Figure 8.

For the lowest switching loss, the switching sequence for the second SVM is as illustrated in Figure 10. Only one switching occurs at each switching state transition except for the one between the zero vector and vector 1 or 4. Figure 10 only shows the sequence for the odd number sectors; for the even number sectors, the sequence from v_1 to v_4 is reversed.

The switching sequence above will not give lowest torque ripple. With v_1 and v_4 ignored, the v_2 and v_3 are two cascaded torque increasing ramps. They can be separated by the zero-vector with certain duty ratio, which can be computed to achieve evenly distributed torque increasing and decreasing ramps, i.e. lowest torque ripple. This sequence reshuffling can be done on the fly for each DSP cycle and be easily integrated into the modulator.

However, the increased control complexity and extra switching loss might be undesirable. For overall optimal vector sequence, the sequence with lowest switching number per cycle might still be preferred unless torque ripple performance is of higher priority in certain applications.

E. Further Comparison Between the two SVM Methods

The second SVM method has four more switching events per DSP cycle than natural sampling SVM. Also it's more complicated to implement in a DSP. However, its d_2-q_2 plane PWM frequency harmonic current amplitude is slightly smaller, since all four vectors located along the outer ring in d_1-q_1 decagon are in the inner ring in the d_2-q_2 decagon (Figure 3). While both SVM methods produce zero average voltage/current in d_2-q_2 , the PWM frequency current

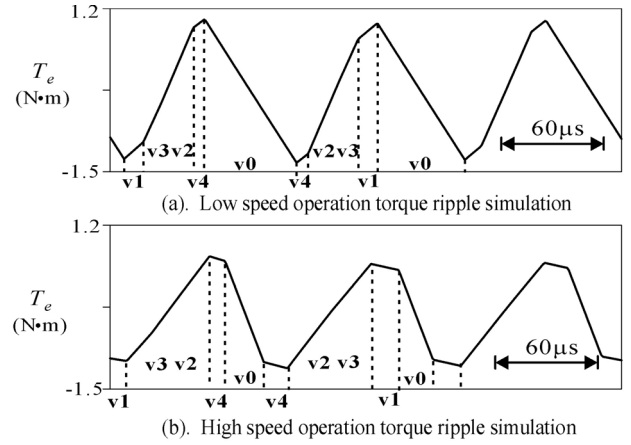


Figure 9. Natural sample SVM torque ripple pattern evolution over speed.

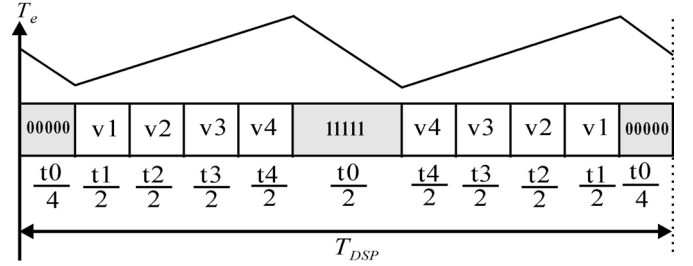


Figure 10. Optimal Switching sequence and resulting torque ripple.

harmonics still exist and are proportional to the amplitudes of the d_2-q_2 voltage vectors used. By comparison, the natural sample SVM uses two mid-ring vectors in d_2-q_2 plane. Therefore higher PWM frequency harmonic currents exist.

VI. SIMULATION RESULTS

A detailed simulation was used to verify the controls presented herein. The induction motor parameters are given in the literature [11] and the PWM carrier frequency was set to 5 kHz.

Figure 11 shows the startup and speed reversal performance of the DTC-SVM in 5-phase induction motor. The three traces from top to bottom are the phase current, electromagnetic torque, and the rotor speed. One set of waveforms are shown since both SVM methods return almost identical results in this time scale. Figure 12 demonstrates dynamic performance. In

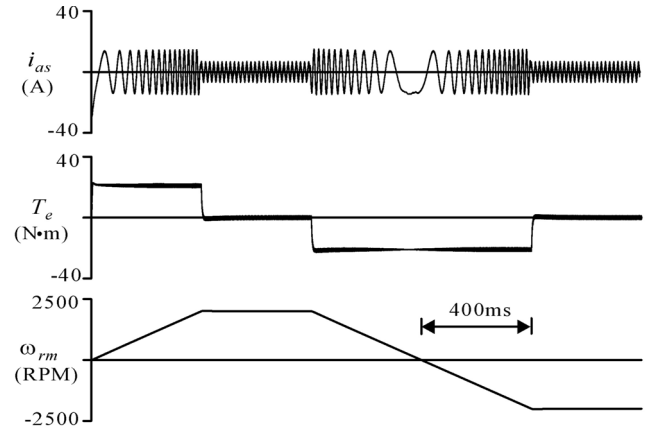


Figure 11. DTC-SVM simulation results (identical results for both SVMs).

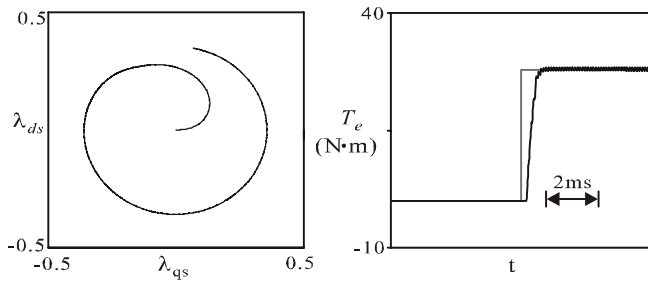


Figure 12. Startup flux locus and torque step response.

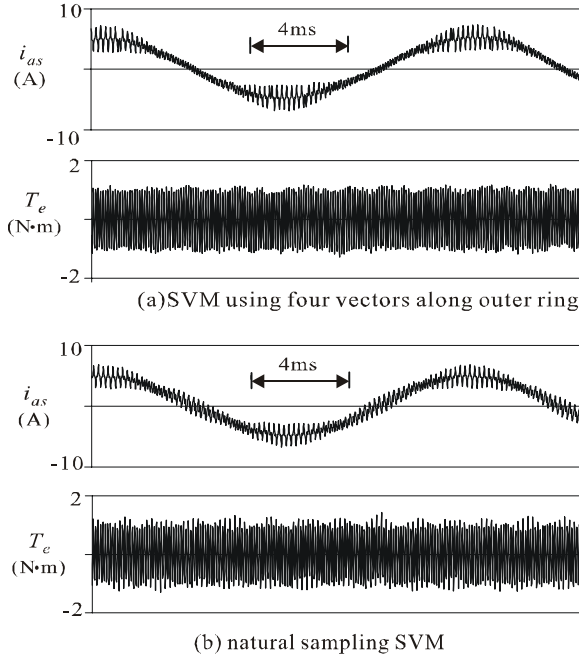


Figure 13. Comparison of phase current and torque between two SVM schemes.

particular, flux build up locus during startup and the step torque command response are shown.

Figure 13 is the comparison of steady-state torque and phase current between the two SVM techniques. Except for the increase in PWM switching components in the natural sampling SVM, the results are similar. Both cases demonstrate sinusoidal waveforms without low frequency harmonics.

VII. CONCLUSION

The traditional lookup table direct torque control (DTC) in 5-phase induction motors with sinusoidally distributed windings suffers from two drawbacks. The first problem is the larger torque ripple when digital hysteresis implementation is used. The second is that the sinusoidally distributed windings in a 5-phase motor have no back-EMF for certain low frequency non-torque producing harmonics and these harmonic voltages can be introduced by the lookup table DTC method and create large harmonic currents. To address these issues, the conventional DTC-SVM is extended into a 5-phase system to improve the steady-state performance. Specifically, this paper introduced two SVM schemes to cancel out all possible low frequency voltage harmonics. To provide a

complete set of solution, the optimal switching sequence is also analyzed. Based on the instantaneous stator flux angle and amplitude variation, the torque ripple pattern evolution and its relationship with the torque ripple reduction are studied in an insightful way. Detailed simulations verify the effectiveness of the DTC-SVM control both in dynamic and steady-state performance.

REFERENCES

- [1] G.S. Buja and M.P. Kazmierkowski, "Direct torque control of PWM inverter-fed AC motors - a survey," *IEEE Transactions on Industrial Electronics*, volume 51, number 4, pages 744-757, August 2004.
- [2] I. Takahashi and Y. Ohmori, "High-performance direct torque control of induction motor," *IEEE Transactions on Industrial Applications*, volume 25, number 2, pages 257-264, 1989.
- [3] X. Xue, X. Xu, T.G. Habetler, and D.M. Divan, "A low cost stator flux oriented voltage source variable speed drive," *Proceeding of the IEEE Industry Applications Society Conference*, volume 1, pages 410-415, 1990.
- [4] T.G. Habetler, F. Profumo, M. Pastorelli, and L.M. Tolbert, "Direct torque control of induction motor using space vector modulation," *IEEE Transactions on Industrial Applications*, volume 28, pages 1045-1053, September/October 1992.
- [5] Y.S. Lai and J.H. Chen, "A new approach to direct torque control of induction motor drives for constant inverter switching frequency and torque ripple reduction," *IEEE Transactions on Energy Conversion*, volume 16, number 3, pages 220-227, September 2001.
- [6] H.A. Toliyat and H. Xu, "A novel direct torque control (DTC) method for five-phase induction machines," *Proceedings of the IEEE Applied Power Electronics Conference*, volume 1, pages 162-168, September 2001.
- [7] L. Parsa and H.A. Toliyat, "Five-Phase Permanent-Magnet Motor Drives," *IEEE Transactions on Industry Applications*, volume 41, number 1, pages 30-37, January/February 2005.
- [8] H.A. Toliyat, "Analysis And Simulation of Five-Phase Variable-Speed Induction Motor Drives Under Asymmetrical Connections," *IEEE Transactions on Power Electronics*, volume 13, number 4, pages 748-756, July 1998.
- [9] Y. Zhao and T.A. Lipo, "Space Vector PWM Control of Dual Three Phase Induction Machine Using Vector Space Decomposition," *IEEE Transactions on Industry Applications*, volume 31, number 5, pages 1100-1109, 1995.
- [10] K.N. Pavithran, R. Parimelagan, and M.R. Krishnamurthy, "Studies on Inverter-Fed Five-Phase Induction Motor Drive," *IEEE Transactions on Power Electronics*, volume 3, number 2, pages 224-235, 1988.
- [11] S. Lu and K.A. Corzine, "Multilevel multi-phase propulsion drives," *Proceedings of the IEEE Electric Ship Technologies Symposium*, pages 363-370, July 2005.



Shuai Lu received BSEE degree from the Chongqing University, China in 1997; and the MSEE degree from the University of Wisconsin - Milwaukee in 2003 and is now pursuing a Ph.D. degree at the University of Missouri - Rolla. His research specialty is power electronics and machine drives. Contact: sl4xf@umr.edu.



Keith A. Corzine received the BSEE, MSEE, and Ph.D. degrees from the University of Missouri - Rolla in 1992, 1994, and 1997 respectively. He taught at the University of Wisconsin - Milwaukee from 1997 to 2004 and is now an Associate Professor at the University of Missouri - Rolla. His research interests include power electronics, motor drives, Naval ship propulsion systems, and electric machinery analysis. Contact: Keith@Corzine.net.